Journal of Musculoskeletal and Neuronal Interactions JMNI

Original Article

Mechanical Stress Via Muscle Contractile Exercise Suppresses Atrophic Alterations of Bone-microstructure in Immobilized Rat Femurs

Yasuhiro Kajiwara[1,2], Yuichiro Honda[1,3], Ayumi Takahashi[1], Natsumi Tanaka[4], Hironobu Koseki[1,3], Junya Sakamoto[1,3], Minoru Okita[1,3]

[1]Department of Physical Therapy Science, Nagasaki University Graduate School of Biomedical Sciences, Nagasaki, Japan;
[2]Department of Rehabilitation, Nagasaki University Hospital, Nagasaki, Japan;
[3]Institute of Biomedical Sciences (Health Sciences), Nagasaki University, Nagasaki, Japan;
[4]Department of Physical Therapy, School of Rehabilitation Sciences, Seirei Christopher University, Shizuoka, Japan

Abstract

Objectives: This study aimed to determine whether mechanical stress via muscle contractile exercise with belt electrode-skeletal muscle electrical stimulation (B-SES) device effectively prevents immobilization-induced bone atrophy. **Methods**: Wistar rats were randomly divided into the control (CON) group, immobilization (IM) group (immobilized treatment only), HES and LES groups (immobilized treatment and high or low-intensity electrical muscular stimulation through B-SES device). Bilateral femurs were used for X-ray micro-CT and biomechanical tests. **Results**: The maximum load value was significantly lower in the IM and HES groups than in the CON group and significantly higher in the LES group than in the IM group. The maximum crushing load was significantly lower in the IM, HES, and LES groups than in the CON group, and significantly higher in the HES and LES groups than that in the IM group. In micro-CT, the mechanical stress by B-SES device did not affect degenerative microstructural changes in the cortical bone, but prevented those changes in the cancellous bone. **Conclusions**: Applying mechanical stress via B-SES device suppressed the loss of cancellous bone density and degenerative microstructural changes caused by immobilization, which in turn suppressed the reduction of bone strength. From these findings, muscle contractile exercise may be effective in preventing immobilization-induced bone atrophy.

Keywords: Bone Microstructure, Bone Strength, Immobilization, Mechanical Stress, Muscle Contractile Exercise

Introduction

Mechanical stress on bones via muscle contraction and loading is essential for maintaining healthy bone homeostasis[1,2]. However, bed rest and cast fixation limit the amount of mechanical stress applied to bone, which can cause immobilization-induced bone atrophy. Loss of bone density and degenerative changes in the bone microstructure occur in immobilization-induced bone atrophy; these lesions are caused by pathological changes in the cortical and cancellous bone[3].

The cortical bone constitutes the dense outer layer in long bone shafts and on the outer surfaces of other bones; it is composed of closely packed osteons (cylinders of bone tissue). Cortical bone is also essential for maintaining the skeletal structure, providing strength and rigidity. Cancellous bone forms a lighter, more porous inner layer and is found at the ends of long bones and within other thicker bones, such as the vertebrae and pelvis. Cancellous bone has a porous structure with a network of tiny spaces filled with bone marrow, which helps to reduce the overall weight of the bone while still providing strength and support. In addition, cancellous bone plays an important role in bone growth and repair under mechanical stress. Pathological alterations of cortical and cancellous bones are related to decreased

The authors have no conflict of interest.

Corresponding author: Minoru Okita, Department of Physical Therapy Science, Nagasaki University Graduate School of Biomedical Sciences, Sakamoto 1-7-1, Nagasaki, Nagasaki 852-8520, Japan
E-mail: mokita@nagasaki-u.ac.jp

Edited by: G. Lyritis
Accepted 4 December 2023

bone strength and an increased risk of fragility fractures[4,5]. Thus, we surmise that applying appropriate mechanical stress to the cortical and cancellous bone at an early stage of immobilization may help reduce immobilization-induced bone atrophy, and prevent subsequent bone fracture.

Muscle contraction induced by electrical stimulation can apply mechanical stress to immobilized bones, and this intervention may be effective in counteracting immobilization-induced bone atrophy. In a previous study, Lam et al. reported that tetanic muscle contraction with an electrical stimulation device was more effective than twitch muscle contraction in regards to increasing bone density and preventing degenerative changes in the bone microstructure[6]. However, electrical stimulation for bone healing is still controversial, as some investigators have shown that it does not affect bone microstructure[7,8]. Thus, results of the effects of electrical stimulation-induced tetanic muscle contraction on immobilization-induced bone atrophy have been inconsistent. As the previous studies referenced above used a monopolar electrode device, sufficient current (power) for muscle contraction may not have been obtained due to the limited size of the electrodes.

A belt electrode skeletal muscle electrical stimulation (B-SES) device (Homer Ion, Tokyo, Japan) was developed as a novel device for electrical stimulation therapy. An advantage of this device is that the entire belt is an electrode that can deliver electricity to the whole lower limb[9]. The usual pattern of tetanic muscle contraction by electrical stimulation occurs with stimulus frequencies of 50–100 Hz in rat skeletal muscles[10,11]. A belt electrode ensures that the skeletal muscles contract simultaneously and thus the bones experience more mechanical stress[12]. Studies have shown that simultaneous muscle tetanic contraction during interval running exercise led to increased bone density, which is related to reducing the risk of bone fractures[13,14]. Although high-intensity exercise is challenging for older patients at a risk of fragility fractures, tetanic muscle contraction using a belt electrode device may be an effective alternative for some patients. We therefore hypothesized that tetanic muscle contraction using a belt electrode can effectively reduce immobilization-induced bone atrophy, and proceeded to test this hypothesis in animal experiments.

Materials and methods

Animals

Eight-week-old male Wistar rats (n = 51) were obtained from CLEA Japan, Inc. (Tokyo, Japan). All rats were housed in 30 × 40 × 20-cm cages (2 rats/cage) and maintained on a 12-h light/dark cycle at an ambient temperature of 25°C. Food and water were provided *ad libitum*. Rats were randomly divided into experimental (n = 38) and control (CON) groups (n = 13). The rats in the control group were maintained without any treatment or intervention. In the experimental group, the bilateral hind limbs were fixed using the immobilization process described in our previous study[15]. Briefly, the animals in the experimental group were anesthetized with the combination of the following anesthetic agents: 0.375 mg/kg medetomidine (Kyoritu Pharma, Tokyo, Japan), 2.0 mg/kg midazolam (Sandoz Pharma Co., Ltd., Tokyo, Japan), and 2.5 mg/kg butorphanol (Meiji Seika Pharma, Tokyo, Japan). The hind limbs of each rat were fixed with plaster casts, and the animals were allowed to recover from anesthesia. The immobilization was kept for two weeks, with the plaster cast replaced daily to prevent hind paw edema. The experimental group was then further divided into the immobilization (IM) group (n=12; with immobilization treatment only), the HES group (n = 13; with immobilization treatment and high-intensity electrical muscular stimulation through B-SES device), and the LES group (n = 13; with immobilization treatment and low-intensity electrical muscular stimulation through B-SES device). All experimental procedures were performed under anesthesia, and all efforts were made to minimize suffering.

Protocol for electrical stimulation through B-SES device

The rats in the HES and LES groups were anesthetized and removed from the casts. Electrical muscle stimulation was applied to bilateral hind limbs using an electrical stimulator for small animals (Homer Ion). The belt electrodes were wrapped around the proximal thigh and distal lower leg, and bilateral lower limb skeletal muscles were subjected to electrical stimulation by B-SES device. In the protocol, the stimulus frequency was 50 Hz, duty cycle was 2 s (do)/ 2 s (rest), and stimulus time was 15 min. Electrical stimulation was applied once a day, six days a week, for two weeks. The stimulus intensity was determined using other rats (n = 2) in the preliminary experiments. The muscle strength of the healthy rat hindlimbs was measured using a force gauge[16]. Next, 100% maximal voluntary contraction (MVC) was determined, and 60% MVC and 20-30% MVC were calculated. Therefore, the HES group was stimulated at 4.7 mA to induce 60% MVC, while the LES group was stimulated at 2.3 mA to inducing 20-30% MVC.

Tissue sampling and preparation

At the end of the experimental period, animals were euthanized by overexposure of CO_2 after inhalation anesthesia. Both femurs were harvested, and unnecessary soft tissues was removed. The bone weight and length of the femurs were measured. Femur length was defined as the maximum distance from the most proximal point at the greater trochanter to the most distal end of the lateral condyle[17]. Afterward, all femurs were immersed in PBS solution tubes and stored at -80°C for later micromorphological and biomechanical analyses.

X-ray micro-computed tomography imaging

The microstructure of the femurs was measured with X-ray micro-computed tomography (CT) imaging using a SkyScan 1272 (Skyscan, Bruker, Belgium). The samples in tubes containing PBS solution were placed vertically in the

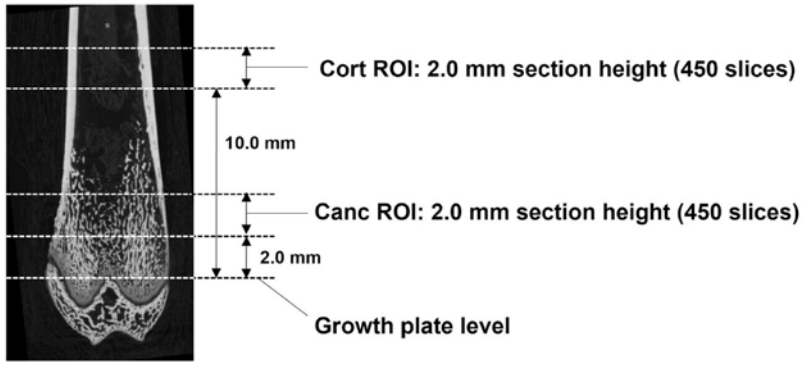

Figure 1. X-ray micro-computed tomography image of rat femur. The cortical region of interest (Cort ROI) and the cancellous region of interest (Canc ROI) begin approximately 10.0 mm and 2.0 mm from the level of the growth plate in the direction of the metaphysis. Each ROI was set at 2 mm and 450 slices were taken.

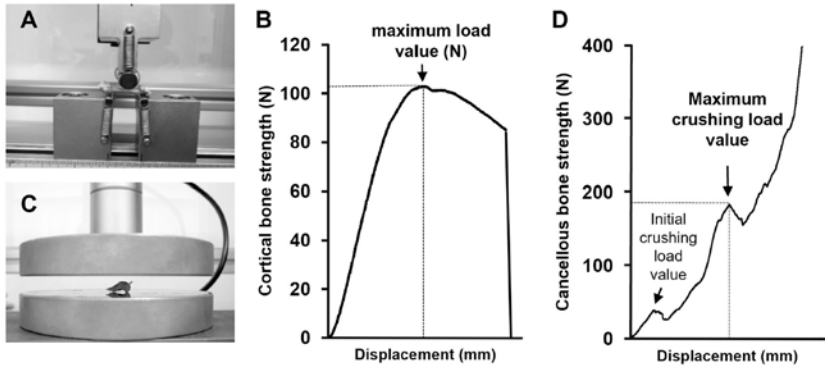

Figure 2. Equipment for biomechanical test and example of measurement results of each test. (A) and (C) indicate the three-point bending strength test and compression test devices. (B) shows a load-displacement plot. The cortical bone strength was taken as the maximum load value (N). (D) demonstrates the compression load-displacement curve. The strength of the cancellous bone was assumed to be the maximum crushing load (N).

sample holder after thawing at 4°C. The X-ray images were acquired using the following settings: X-ray tube potential 70 kV, X-ray tube current 140 µA, 1.0 mm aluminum filter, pixel size 21.5 µm, exposure time 1891 ms, rotation step 1.0°, and tomographic rotation 360°. After the images were reconstructed using NRecon software (Skyscan, Bruker, Belgium), smoothing, misalignment compensation, ring artifact correction, and 25% beam-hardening correction were applied. The images were then analyzed using the CTAn software (Skyscan, Bruker, Belgium). The cortical region of interest (Cort ROI) was selected approximately 10.0 mm from the growth plate level toward the metaphyseal trunk and extended an additional 2.0 mm from this location (450 slices) (Figure 1). The total cross-sectional area inside the periosteal envelope (Tt.Ar, mm^2); cortical bone area (Ct.Ar, mm^2); average cortical thickness (Ct.Th, µm); and polar moment of inertia (pMOI, mm^4) were calculated. The cancellous region of interest (Canc ROI) was defined as starting about 2.0 mm from the growth plate level in the direction of the metaphysis (Figure 1) and extended from this position for a further 2.0 mm (450 slices). For this ROI the ratio of the segmented bone volume to the total volume (BV/TV, %), structure model index (SMI), mean trabecular thickness (Tb.Th, µm), trabecular number (Tb.N, 1/mm), trabecular separation (Tb.Sp, µm), connectivity density (Conn.Dens, $1/mm^3$), and degree of anisotropy (DA) were calculated. The estimated mineral densities of the cortical and

Table 1. Bone weight, bone length, and weight/length ratio.

	CON	IM	HES	LES
Bone weight (mg)	875.0 ± 92.6	757.7 ± 75.9*	759.5 ± 63.0*	795.1 ± 42.5*
Bone length (mm)	34.5 ± 1.0	33.0 ± 1.0*	32.6 ± 0.7*	32.9 ± 0.5*
Weight/length ratio (mg/mm)	25.4 ± 2.4	23.0 ± 2.3*	23.3 ± 1.9*	24.2 ± 1.3

**, Significant difference (p < 0.05) compared with the CON group.*

Table 2. Outcomes for cortical bone morphology.

	CON	IM	HES	LES
TMD (%)	59.5 ± 6.2	60.9 ± 7.2	59.1 ± 6.5	60.5 ± 3.6
Tt.Ar (mm^2)	10.8 ± 1.1	9.5 ± 0.8*	9.4 ± 0.7*	9.6 ± 0.7*
Ct.Ar (mm^2)	6.3 ± 0.5	5.7 ± 0.7*	5.5 ± 0.4*	5.8 ± 0.4*
Ct.Th (μm)	528.4 ± 44.7	486.9 ± 47.7*	482.6 ± 26.2*	469.5 ± 35.0*
pMOI (mm^4)	15.6 ± 2.9	12.2 ± 1.8*	11.9 ± 1.6*	12.7 ± 1.7*

*TMD: tissue mineral density in cortical bone; Tt.Ar: total cross-sectional area inside a periosteal envelope; Ct.Ar: cortical bone area; Ct.th: average cortical thickness; pMOI: polar moment of inertia. *, Significant difference (p < 0.05) compared with the CON group.*

trabecular tissues were each calculated and defined as the cortical bone tissue mineral density (TMD) and cancellous bone mineral density (BMD); based upon the measured CT values according to the methodology provided by Skyscan. The TMD and BMD absolute values were determined by comparisons with the two hydroxyapatite phantoms (0.25 and 0.75 g/cm^3 HA BMD phantoms, SkyScan) as density references.

Biomechanical tests

After micro-CT imaging, the bone strength of the samples was measured using a precision universal testing machine (Autograph AG-X; Shimadzu, Kyoto, Japan). The strength of the cortical bone was measured using a three-point bending strength test with a length span of 20 mm between the support points (Figure 2A). A bending force was applied at a uniform speed of 5 mm/min until a fracture occurred. The data was converted into a load-displacement plot. The maximum load value (N) was used as the cortical bone strength (Figure 2B). The strength of the cancellous bone was measured using a compression test (Figure 2C). The distal femur fragment was placed at the center of the plate and compressed at a speed of 5 mm/min until fracture occurred. The compression load-displacement curve rose slowly to the initial crushing load value, at which point failure occurred. Following initial failure, the plot continued to rise and indicated second failure. The maximum crushing load value (N), which is the loading value required for the second failure, was adopted as the strength of the cancellous bone (Figure 2D).

Statistical analysis

All data is presented as the mean ± standard deviation. Differences between groups were assessed using one-way analysis of variance (ANOVA) followed by Scheffe's method. Differences were considered statistically significant at $p < 0.05$.

Results

Bone weight and bone length

The bone weight and femur length were significantly lower in the IM, HES, and LES groups compared to the CON group. In addition, the weight/length ratio was significantly lower in the IM and HES groups than that in the CON group, and there was no significant difference between the CON and LES groups (Table 1).

Bone microstructure from micro-CT

Micro-CT images of the cortical bone in the mid-diaphysis of the femur showed that the cortical bone in the experimental groups was thinner than that in the CON group, and there were no significant changes in bone microstructure between the experimental groups (Figure 3A-D). TMD was not different among the groups, and the Tr,Ar, Ct.Ar, Ct.th, and pMOI in the IM, HES, and LES groups were significantly lower than those in the control group (Table 2).

Although micro-CT images of the cancellous bone in the distal metaphysis of the femur showed that the bone trabeculae were less dense in the three immobilized groups

Table 3. Outcomes for cancellous bone microarchitecture.

	CON	IM	HES	LES
BMD (%)	29.9 ± 3.4	20.8 ± 2.8*	23.7 ± 2.8*#	25.0 ± 3.7*#
BV/TV (%)	39.8 ± 5.1	30.1 ± 4.4*	34.5 ± 4.5*#	35.6 ± 5.1*#
SMI	1.3 ± 0.5	1.8 ± 0.2*	1.6 ± 0.3	1.6 ± 0.4
Tb.Th (μm)	116.1 ± 12.9	101.0 ± 4.4*	104.2 ± 3.9*	100.9 ± 7.6*
Tb.N (1/mm)	3.4 ± 0.3	3.0 ± 0.4*	3.3 ± 0.4#	3.5 ± 0.4#
Tb.Sp (μm)	171.8 ± 29.3	205.8 ± 50.0*	178.1 ± 23.9#	143.7 ± 18.7*#†
Conn.Dens (1/mm^3)	143.8 ± 27.8	101.2 ± 20.1*	124.3 ± 19.0#	155.2 ± 33.9#†
DA	1.6 ± 0.1	1.8 ± 0.2*	1.8 ± 0.1*	1.5 ± 0.1#†

*BMD: bone mineral density in cancellous bone; BV/TV: the ratio of the segmented bone volume to the total volume; SMI: structure model index; Tb.Th: mean trabecular thickness; Tb.N: trabecular number; Tb.Sp: trabecular separation (mm); Conn.Dens: connectivity density; DA: degree of anisotropy. *, Significant difference (p < 0.05) compared with the CON group. #, Significant difference (p < 0.05) compared with the IM group. †, Significant difference (p < 0.05) compared with the HES group.*

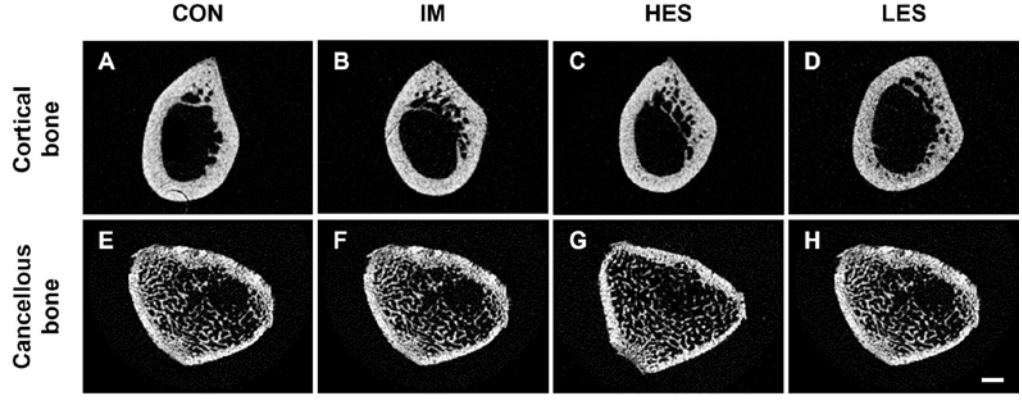

Figure 3. Micro-computed tomography image of the cortical bone and cancellous bone. (A-D) show the images of the cortical bone in the femoral mid-diaphysis, (E-H) indicate the images of the cancellous bone in the femoral distal metaphysis. (A, E) represent the CON group, (B, F) represent the IM group, (C, G) represent the HES group, and (D, H) represent the LES group. The scale bar demonstrates 2.0 mm.

than in the CON group, they were slightly thicker in the HES and LES groups than in the IM group (Figure 3E-H). In Table 3, the BMD and BV/TV in the IM, HES, and LES groups were significantly lower than those in the CON group, and those in the HES and LES groups were significantly higher than those in the IM group. SMI in the IM group was significantly higher than that in the CON group, while the HES and LES groups had no significant difference compared to the CON group. The Tb.Th in the IM, HES, and LES groups was significantly lower than that in the CON group; there was no significant difference between the IM, HES, and LES groups. Tb.N in the IM group was significantly lower than that in the CON group, and Tb.N in the HES and LES groups was significantly higher than that in the IM group. Tb.Sp in the IM group was significantly higher than that in the CON group, and was significantly lower in the HES and LES groups than in the IM group. Also, the Tb.Sp in the LES group was significantly lower than the HES group. The Conn.Dens in the IM group was significantly lower than that in the CON group, and the Conn.Dens in the HES and LES groups was significantly higher than that in the IM group. In the comparison of these two groups, the Conn.Dens in the LES group was significantly lower than that in the HES group. The DA in the IM and HES groups was significantly higher than that in the CON group, and the DA in the LES group was significantly lower than that in the IM and HES groups.

Bone strength as determined by biomechanical tests

The results of the three-point bending tests are presented in Figure 4A. The average maximum load value (N) was 110.0 ± 9.0 in the CON group two weeks after immobilization. The

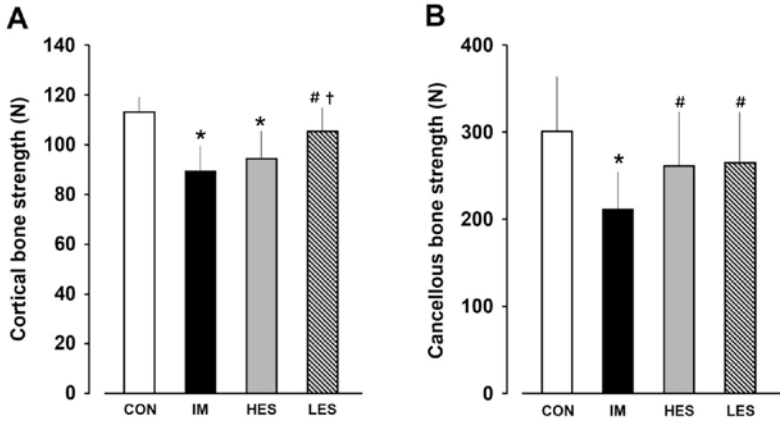

Figure 4. Results of cortical and cancellous bone strength. (A) indicates the result of cortical bone strength from the three-point bending strength test. (B) shows the cancellous bone strength from the compression test. Open bars represent the CON group. Black bars represent the IM group. Gray bars represent the HES group. Hatched bars represent the LES group. Data are presented as mean ± standard deviation. *, Significant difference ($p < 0.05$) compared with the CON group. #, Significant difference ($p < 0.05$) compared with the IM group. †, Significant difference ($p < 0.05$) compared with the HES group.

maximum load values (N) in the IM, HES, and LES groups were 88.0 ± 12.9, 94.8 ± 11.6, and 105.9 ± 10.9, respectively. The maximum load was significantly lower in the IM and HES groups compared with the CON group. However, the maximum load was significantly higher in the LES group than in the IM and HES groups. The maximum crushing load is shown in Figure 4B. The mean maximum crushing load value (N) was 299.7 ± 64.0 in the CON group. In the IM, HES, and LES groups, the maximum crushing load value (N) was 211.9 ± 43.4, 262.8 ± 63.5, and 264.9 ± 59.3, respectively, at two weeks following immobilization. The maximum crushing load was significantly lower in the IM group than in the CON group. However, the maximum crushing load was significantly higher in the HES and LES groups than in the IM group. There were no significant differences between the two B-SES application groups.

Discussion

This study investigated the changes in bone strength, density, and microstructure of the cortical and cancellous bone regions in immobilized femurs. Bone weight, bone length, and weight/length ratio were significantly lower in the IM group than in the CON group, and previous research showed that bone weight and length were reduced in atrophic femurs[18,19]. These results are similar to those of previous studies, and it was therefore concluded that the bone atrophy model used in this study is analogous to past studies.

Cortical bone is a significant contributor to the mechanical strength of long bones, and accounts for nearly 80% of the total skeletal mass. Healthy cortical homeostasis is maintained by the application of mechanical stimulation during normal activity[20]. Cortical bone homeostasis is maintained by a balance between proper bone formation and resorption; disruption of this balance leads to adverse changes in the cortical bone microstructure[21]. A previous study indicated that decreased mechanical stimulation reduces bone formation and increases cortical bone resorption, resulting in weakening of the cortical bone microstructure[21]. In the micro-CT analyses in this study, the Tt.Ar, Ct.Ar, Ct.Th, and pMOI in the IM group were significantly lower than those in the CON group, indicating thinning of the cortical bone and decreased resistance to torsional forces. In addition, the tested cortical bone strength in the IM group was significantly lower than that in the CON group. From these results, we surmised that the immobilized femoral cortical bone underwent degenerative changes in its microstructure, which were responsible for the loss of cortical bone strength.

Cancellous bone is a stratified, spongy, and porous material composed of hard and soft tissues in the epiphyseal and metaphyseal regions of long bones. Macroscopically, the hard trabecular meshwork provides a stiff and ductile structure that frames the soft, highly cellular marrow that fills the intertrabecular spaces. At the microscopic level, the microstructure of the trabecular meshwork is organized to optimize load transfer[2,22,23]. Much like cortical bone, consistent mechanical stimulation regulates the balance between the formation and resorption of cancellous bone. A reduction in mechanical stimulation similarly contributes to inappropriate changes in the cancellous bone microstructure[24]. In the present study, the BMD in the IM group was significantly lower than that in the CON group, and the bone density in the cancellous bone of the femur decreased with immobilization. In addition, the BV/TV, Tb.Th, Tb.N, and Conn.Dens in the IM group were significantly lower than those in the CON group,

and these results showed a decrease in the number of bone trabeculae, thinning of the trabeculae, and disruption of the connectivity of the trabeculae in cancellous bone. Moreover, the SMI, Tb.Sp, and DA in the IM group were significantly higher than those in the CON group, indicating that bone resorption occurs preferentially in bone trabeculae that run in directions other than the direction of principal stress[25]. Therefore, decreased bone density and degenerative microstructural changes occurred in the cancellous bone of immobilized rat femurs, which is likely responsible for the reduction in the maximum crushing load of the cancellous bone.

Exercise such as walking typically induces mechanical stress on bones, which contributes to the maintenance and improvement of bone strength, and its beneficial effects have been observed in cancellous bone[26,27]. However, it is difficult for the bones to experience mechanical stress through exercise when patients are confined to bed rest for medical procedures. As an alternative, previous studies have reported that mechanical stress on the bone through muscle contractile exercise increases cancellous bone strength[28]. One potential method for producing muscle contraction exercises is the use of electrical stimulation. Electrical stimulation via B-SES device can contract multiple skeletal muscles simultaneously[9] and may be able to apply more mechanical stress to bones than conventional electrical stimulation devices. In this study, the HES and LES groups were observed to have improved cancellous bone strength compared to the IM group. These results were similar to those of previous studies that investigated the effects of exercise on bone atrophy. Mechanical stress from walking has been reported to improve BMD in atrophic cancellous bones[29]. In this study, BMD improvement in the femur was significantly greater in the HES and LES groups than that in the IM group. Therefore, although BMD was reduced in bones with atrophic changes due to immobilization, application of mechanical stress appears to be effective in preventing BMD decline.

The bone weight and length results showed that mechanical loading by B-SES device did not affect the weight or length of the immobilized femur. Furthermore, the application of mechanical stress by muscle contractile exercise using electrical stimulation showed no changes in cortical bone architectural markers. However, it improved cancellous bone architectural markers such as BV/TV, Tb.Th, Tb.N, and Tb.Sp. Immobilization-induced degenerative changes in the femoral microstructure were suppressed in the HES and LES groups.

Conventional monopolar electrodes induce muscle contractile exercise only in a narrow range, and mechanical stress loading on bone is localized. Therefore, previous studies did not provide consistent views on whether muscle contractile exercises using electrical stimulation with monopolar electrodes were beneficial in suppressing degenerative bone alterations[6-8]. However, the belt electrode used in B-SES device can induce muscle contractile exercise in the entire lower limb[9]. Additionally, previous studies indicated that wide-range muscle contractile exercises like walking and running, etc. were beneficial for maintaining and improving cancellous bone strength[26,27]. Our experiment showed that mechanical stress loading using the B-SES device suppressed the degenerative changes and decreased bone strength in the cancellous bone. Therefore, we surmised that the belt electrode solves the problems of conventional monopolar electrodes and applying mechanical stress via B-SES device is an effective therapeutic strategy for immobilization-induced bone atrophy. Moreover, the LES group might be similarly effective to the HES group in suppressing degenerative bone changes of cancellous bones by immobilization. These results indicate that low-intensity muscle contractile exercise (20-30% MVC) may have similar effects to high-intensity muscle contractile exercise (60% MVC) in suppressing immobilization-induced bone atrophy. In clinical rehabilitation, some patients cannot perform high-intensity muscle contraction exercises due to postoperative pain, etc.; such patients are often provided with low-intensity muscle contraction exercises. Therefore, we surmised that the results of this study will assist in developing treatment strategies for patients who may suffer from immobilization-induced bone atrophy.

This study had several limitations. First, it remains to be determined whether the current electrical stimulation protocol is the most effective intervention. Further examination of various frequencies, intensities, duty cycles, times, and intraday sessions of electrical stimulation protocols is required. Additionally, we were unable to determine why muscle contractile exercise through B-SES device only affected cancellous bone. Since the dynamics of osteoblastic and osteoclastic cells involved in bone formation and resorption, respectively, play a role in the remodeling of bone trabeculae, histological analysis of these cells in cancellous bone should be performed in the future. Furthermore, the LES group might be more effective than the HES group in Tb.Sp, Conn.Dens, and DA. However, no previous studies have examined these points, and the biological mechanism has not been clarified. These points are for further study.

In summary, the mechanical stress via tetanic muscle contraction induced by B-SES device suppressed the decrease in cancellous bone density and degenerative microstructural changes caused by immobilization. These beneficial changes prevented the decline in bone strength. Based on these results, muscle contractile exercise using electrical stimulation may be an effective therapeutic strategy for preventing immobilization-induced bone atrophy.

Ethics approval

The Ethics Review Committee of Nagasaki University approved the experimental protocol for animal experimentation (approval no. 1903281524).

Acknowledgments

Homer Ion Co., Ltd. (Tokyo, Japan) provided a belt electrode skeletal muscle electrical stimulation system for small animals. We would like to thank Alexander Burden, Jeffery Barrett, and Prof. Thomas Oxland (ICORD, Blusson Spinal Cord Centre, 818 West 10th Avenue, Vancouver, BC, V5Z 1M9, Canada) as English editors.

Authors' contributions

Study conception and design: Y.K., H.K., J.S., and M.O.; Data analysis and interpretation: Y.K., Y.H., A.T., N.T., H.K., and M.O.; Article drafting: Y.K., Y.H., and M.O.; Critical revision of the article for important intellectual content: Y.K., Y.H., J.S. and M.O.; Statistical expertise: Y.H. and M.O.; Obtaining funding: M.O.; and Data collection and assembly: Y.K., Y.H. and M.O. All authors approved the final version of the manuscript.

Funding

This study was supported by the Japan Society for the Promotion of Science (KAKENHI, Grant No. 21HO3291) and ALCARE Co., Ltd. (Tokyo, Japan) and Homer Ion Co., Ltd.

References

1. Schaffler MB, Cheung W-Y, Majeska R, Kennedy O. Osteocytes: Master Orchestrators of Bone. Calcif Tissue Int 2014;94(1):5-24.
2. Mullender MG, Huiskes R. Proposal for the regulatory mechanism of Wolff's law. J Orthop Res 1995;13(4):503-12.
3. Koseki H, Osaki M, Honda Y, Sunagawa S, Imai C, Shida T, Matsumura U, Sakamoto J, Tomonaga I, Yokoo S, Mizukami S, Okita M. Progression of microstructural deterioration in load-bearing immobilization osteopenia. PLoS One 2022;17(11):e0275439.
4. Hart NH, Nimphius S, Rantalainen T, Ireland A, Siafarikas A, Newton RU. Mechanical basis of bone strength: influence of bone material, bone structure and muscle action. J Musculoskelet Neuronal Interact 2017;17(3):114-39.
5. Rolvien T, Amling M. Disuse Osteoporosis: Clinical and Mechanistic Insights. Calcif Tissue Int 2022;110(5):592-604.
6. Lam H, Qin YX. The effects of frequency-dependent dynamic muscle stimulation on inhibition of trabecular bone loss in a disuse model. Bone 2008;43(6): 1093-100.
7. Inoue S, Hatakeyama J, Aoki H, Kuroki H, Niikura T, Oe K, Fukui T, Kuroda R, Akisue T, Moriyama H. Effects of ultrasound, radial extracorporeal shock waves, and electrical stimulation on rat bone defect healing. Ann N Y Acad Sci 2021;1497(1):3-14.
8. Inoue S, Hatakeyama J, Aoki H, Kuroki H, Niikura T, Oe K, Fukui T, Kuroda R, Akisue T, Moriyama H. Utilization of Mechanical Stress to Treat Osteoporosis: The Effects of Electrical Stimulation, Radial Extracorporeal Shock Wave, and Ultrasound on Experimental Osteoporosis in Ovariectomized Rats. Calcif Tissue Int 2021;109(2):215-29.
9. Numata H, Nakase J, Inaki A, Mochizuki T, Oshima T, Takata Y, Kinuya S, Tsuchiya H. Effects of the belt electrode skeletal muscle electrical stimulation system on lower extremity skeletal muscle activity: Evaluation using positron emission tomography. Journal of Orthopaedic Science 2016;21(1):53-6.
10. Honda Y, Takahashi A, Tanaka N, Kajiwara Y, Sasaki R, Okita S, Sakamoto J, Okita M. Muscle contractile exercise through a belt electrode device prevents myofiber atrophy, muscle contracture, and muscular pain in immobilized rat gastrocnemius muscle. PLoS One 2022;17(9):e0275175.
11. Yoshida N, Morimoto Y, Kataoka H, Sakamoto J, Nakano J, Okita M. Effects of Combination Therapy of Heat Stress and Muscle Contraction Exercise Induced by Neuromuscular Electrical Stimulation on Disuse Atrophy in the Rat Gastrocnemius. J Phys Ther Sci 2013;25(2):201-6.
12. Boudenot A, Achiou Z, Portier H. Does running strengthen bone? Applied Physiology, Nutrition, and Metabolism 2015;40(12):1309-13.
13. Bréban S, Benhamou C-L, Chappard C. Dual-Energy X-ray Absorptiometry Assessment of Tibial Mid-third Bone Mineral Density in Young Athletes. Journal of Clinical Densitometry 2009;12(1):22-7.
14. Schott AM, Cormier C, Hans D, Favier F, Hausherr E, Dargent-Molina P, Delmas PD, Ribot C, Sebert JL, Breart G, Meunier PJ. How Hip and Whole-Body Bone Mineral Density Predict Hip Fracture in Elderly Women: The EPIDOS Prospective Study. Osteoporosis International 1998;8(3):247-54.
15. Honda Y, Sakamoto J, Nakano J, Kataoka H, Sasabe R, Goto K, Tanaka M, Origuchi T, Yoshimura T, Okita M. Upregulation of interleukin-1β/transforming growth factor-β1 and hypoxia relate to molecular mechanisms underlying immobilization-induced muscle contracture. Muscle & Nerve 2015;52(3):419-27.
16. Honda Y, Tanaka N, Kajiwara Y, Kondo Y, Kataoka H, Sakamoto J, Akimoto R, Nawata A, Okita M. Effect of belt electrode-skeletal muscle electrical stimulation on immobilization-induced muscle fibrosis. PLoS One 2021;16(5):e0244120.
17. Foster AD. The impact of bipedal mechanical loading history on longitudinal long bone growth. PLoS One 2019;14(2):e0211692.
18. Williams JA, Windmill JFC, Tanner KE, Riddell JS, Coupaud S. Global and site-specific analysis of bone in a rat model of spinal cord injury-induced osteoporosis. Bone Reports 2020;12:100233.
19. Zhang S, Ueno D, Ohira T, Kato H, Izawa T, Yamanouchi S, Yoshida Y, Takahashi A, Ohira Y. Depression of Bone Density at the Weight-Bearing Joints in Wistar Hannover Rats by a Simulated Mechanical Stress Associated With Partial Gravity Environment. Frontiers in Cell and Developmental Biology 2021;9:707470.
20. Coulombe JC, Senwar B, Ferguson VL. Spaceflight-Induced Bone Tissue Changes that Affect Bone Quality and Increase Fracture Risk. Curr Osteoporos Rep 2020;18(1):1-12. Vico L, Hargens A. Skeletal changes during and after spaceflight. Nature Reviews Rheumatology 2018;14(4):229-46.
21. Vico L, Hargens A. Skeletal changes during and after spaceflight. Nature Reviews Rheumatology

2018;14(4):229-46.
22. Oftadeh R, Perez-Viloria M, Villa-Camacho JC, Vaziri A, Nazarian A. Biomechanics and Mechanobiology of Trabecular Bone: A Review. J Biomech Eng 2015;137(1):0108021-01080215.
23. Bayraktar HH, Morgan EF, Niebur GL, Morris GE, Wong EK, Keaveny TM. Comparison of the elastic and yield properties of human femoral trabecular and cortical bone tissue. Journal of Biomechanics 2004;37(1):27-35.
24. Coupaud S, McLean AN, Purcell M, Fraser MH, Allan DB. Decreases in bone mineral density at cortical and trabecular sites in the tibia and femur during the first year of spinal cord injury. Bone 2015;74:69-75.
25. Ozasa R, Saito M, Ishimoto T, Matsugaki A, Matsumoto Y, Nakano T. Combination treatment with ibandronate and eldecalcitol prevents osteoporotic bone loss and deterioration of bone quality characterized by nano-arrangement of the collagen/apatite in an ovariectomized aged rat model. Bone 2022;157:116309.
26. Westerlind KC, Wronski TJ, Ritman EL, Luo ZP, An KN, Bell NH, Turner RT. Estrogen regulates the rate of bone turnover but bone balance in ovariectomized rats is modulated by prevailing mechanical strain. Proc Natl Acad Sci U S A 1997;94(8):4199-204.
27. Westerlind KC, Fluckey JD, Gordon SE, Kraemer WJ, Farrell PA, Turner RT. Effect of resistance exercise training on cortical and cancellous bone in mature male rats. Journal of Applied Physiology 1998;84(2):459-64.
28. Swift JM, Gasier HG, Swift SN, Wiggs MP, Hogan HA, Fluckey JD, Bloomfield SA. Increased training loads do not magnify cancellous bone gains with rodent jump resistance exercise. J Appl Physiol (1985) 2010;109(6):1600-7.
29. Berman AG, Hinton MJ, Wallace JM. Treadmill running and targeted tibial loading differentially improve bone mass in mice. Bone Rep 2019;10:100195.